Geofluids (2007) 7, 209–226 doi:10.1111/j.1468-8123.2007.00176.x

Changes in sub-water table fluid flow at the end of the Proterozoic and its implications for gas pulsars and MVT lead–zinc deposits

L. M. CATHLES III
Cornell University, Ithaca, NY, USA

ABSTRACT

A fundamental change in the nature of sub-water table fluid flow occurred at roughly the Proterozoic–Phanerozoic boundary when organic matter began to be buried in sufficient quantities that nonaqueous fluids could occupy a significant fraction of the pore space. This allowed the formation of remarkably durable capillary seals that could trap gas in large portions (hundreds of kilometers) of a basin for hundreds of millions of years. Gas loss from these gas zones can be highly dynamic, especially during gas generation. Under the right circumstances, hundreds of cubic kilometers of gas can be rapidly discharged into adjacent permeable aquifers. In Pennsylvanian/Permian time, the Arkoma Basin may have repeatedly discharged such volumes of gas into the very permeable Cambrian sandstone and karstic carbonate aquifers of the mid-continent of the United States. This could have displaced brines rapidly enough to form the Mississippi Valley-type (MVT) lead–zinc deposits of this age that are associated with the Arkoma Basin, heating them only briefly as required by maturity indicators. Sea level rise accompanying the melting of Permian continental glaciers may have triggered the gas expulsion events. This radically new mechanism for the formation of MVT deposits is just one example of the nonlinear dynamics of gas accumulations that are possible since Late Proterozoic time.

Key words: basin centered gas, capillary seals, gas pulsars, glaciation, MVT lead–zinc deposits, Proterozoic

Received 26 July 2006; accepted 8 February 2007

Corresponding author: Lawrence M. Cathles, Cornell University, Ithaca, NY 14853, USA.
Email: lmc19@cornell.edu. Tel: 607-255-2844. Fax: 607-254-4780.

Geofluids (2007) 7, 209–226

INTRODUCTION

The Amitsoq gneiss in Quilangarssuit, Greenland, and the supracrustal rocks associated with it, show that the physical processes that drive aqueous fluids in the earth's crust today have been present since shortly after the Earth was formed. The metamorphosed volcanics, sediments, banded ironstones and conglomerates found in this area have been radiometrically dated at >3.7 Ga (Faure 1977, p. 110). This indicates that before this time magmas invaded the crust and erupted, and water flowed across the surface transporting dissolved and bedload material and causing sediments to accumulate. Thus, from before 3.7 Ga, evaporation left residual brines, precipitation on uplands sourced the gravitational flow of water across and through the surface, compaction occurred where sediments accumulated or were deformed, fluids were released from magmas, and magmatic heat convected adjacent pore waters. All of the physical processes that operate to circulate aqueous fluids through the subsurface today were in operation since the very dawn of Earth history. Subsurface hydrology may therefore have consisted of variations on the same themes. Changes in process intensity and the mix of processes might have attended changes in the rate of seafloor spreading or subduction, rifting and collision events, and the arrival of plume heads at the surface. The scale of subcrustal fluid flow might have changed as supercontinents assembled and fragmented. The chemistry of the fluids certainly changed as the atmosphere became oxygenated. But the basic physical processes driving subsurface aqueous fluid flow could have remained the same across essentially all of earth history.

I argue here that this was not the case because very important new physical processes were introduced at roughly the Proterozoic/Phanerozoic boundary, when organic matter began to be buried in sufficient quantities

that nonaqueous fluids could occupy a significant fraction of the sub-water table pore space. When this happened, capillary forces between the aqueous and nonaqueous fluids re-wrote the rules of sub-water table fluid flow. For the first time, extraordinarily durable seals could form that were capable of trapping gas in basins for hundreds of millions of years. The dynamics of these gas-filled basins allowed large volumes of gas to be expelled very quickly (gas pulsars), and when these entered adjacent permeable aquifers large volumes of brine were displaced. The brine pulses produced a new kind of lead–zinc deposit not seen before; the kind we call Mississippi Valley-type (MVT). Gas-filled basins can be dynamic during, and for about 60 Ma after, periods of rapid sediment accumulation, and perhaps particularly when continental glaciers melt. The purpose of this paper is to make the case for these statements – to describe the evidence that suggests them, the physics that underlies them, and the predictions that can be derived from them, and to show how these predictions relate to a most problematic kind of crustal fluid flow that is associated with the formation of MVT deposits. This is done below by first describing how gas pulsars might operate, then reviewing the enigmatic nature of MVT deposits, and finally making the case that gas pulsars might be responsible for the formation of MVT lead–zinc deposits beginning in Late Proterozoic time.

THE OPERATION OF GAS PULSARS

Gas-filled basins

A gas-filled basin is the essential ingredient of a dynamic gas pulsar. As reviewed recently by Law (2002), the presence of pervasive gas in basins has been noticed at least since Silver (1950) described salient aspects of this phenomenon in the San Juan basin in New Mexico. Appreciation of the broad distribution and economic significance of gas-filled basins began when Masters' (1979, 1984) discovered, explored, and developed gas-filled portions of the Western Canada Sedimentary Basin (WCSB) in Alberta. Masters' (1984) description of the gas-filled parts of the WCSB, that extend over an area that is 500 km long and approximately 100 km wide, remains one of the best introductions to this subject. As he describes, it is not possible to drill a well in this area that does not hit gas, and the exploration challenge is to find 'sweet spots' permeable enough for the ubiquitous gas to be produced. This is quite different from the conventional exploration challenge of finding isolated pockets of trapped gas. In gas-filled parts of the WCSB the pores of both sands and shales are filled with gas. There is very little or no free water, and little or no water is produced during gas production. The gas has no water leg underlying it. The gas is underpressured with respect to hydrostatic conditions as shown in Fig. 1, not overpressured as it is in conventional gas reservoirs. The gas in the WCSB seems to have simply displaced all the water in a large part of the basin. Sixty million years after its generation it remains trapped there, surrounded, but not invaded by, water.

Pervasive gas accumulations, now known as basin-centered gas, are already being exploited and have great potential for increased utilization as a source of natural gas. There are many documented examples in North America, and from these we know that basin-centered gas can be either overpressured, as it is in the Greater Green River, Wind River, Big Horn and Piceance basins, or underpressured, as it is in the Western Canada, San Juan, Denver, Arkoma, and Appalachian basins (Law 2002). The simplest view, and the one adopted here (also see Cathles & Adams 2005), is that overpressured gas displaced the pore waters as it was generated, and later fracturing allowed some of the gas to escape, and depressurized that which remained. This left the top of the gas-saturated zone at hydrostatic pressure and the underlying portions underpressured, as illustrated in Fig. 1. The permeability of the under-pressured basin-centered gas zones is known to be from 1 to 10 microdarcies from extensive production testing

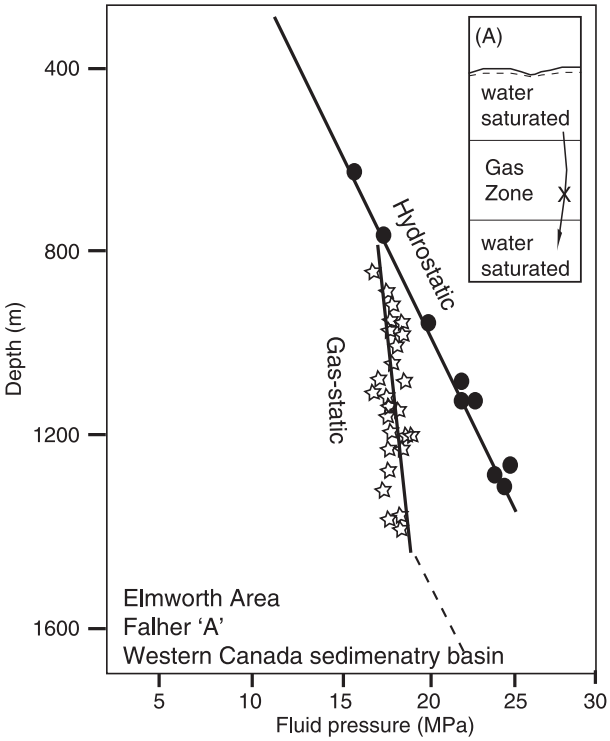

Fig. 1. Fluid pressures measured near the Elmworth gas field in Alberta, Canada from Davis (1984). The top of the gas zone is at hydrostatic pressure. At greater depth the gas is underpressured with respect to hydrostatic. As shown in insert (A), the key to this kind of pressure profile is the absence of a hydrologic connection between the water-saturated zones above and below the gas zone.

in the Appalachian Basin (De Witt 1986). Other basins with under-pressured basin-centered gas have permeability typically <0.1 millidarcies (Law 2002).

Capillary seals

The gas filling the Arkoma, Appalachian, and many other basins has remained in an underpressured or overpressured (and sometimes a mixed) state for hundreds of millions of years. How are these pressures retained for so long? The answer to anomalous pressure retention across hundreds of millions of years is the remarkable healing capacity of capillary seals. Capillary seals are also the second essential component of gas pulsars.

Capillary forces arise when more than one fluid phase is present in the pore space of sediment. These forces are large, and greatly affect fluid flow. The basic principles are simple and have been understood for a long time (see Muskat 1937). Capillary forces pull the phase that wets the sediment (almost always water) into the finer pores of the sediment. The nonwetting phase is ejected from the fine pores and accumulates in the larger ones. Capillary forces are strong. Fine pores can 'suck' water with a force of more than 4 MPa (40 atmospheres). Because the distance between fine and coarse pores is very short, capillary pressure gradients are *far* greater than any of the other pressure gradients driving flow in the subsurface. Capillary forces thus determine the distribution of phases in the pores.

Each phase blocks the flow of the other as if it were rock. A fully water-saturated sediment is impermeable to gas, for example, because the gas has no connected channels of gas through which it can flow. A sediment is most permeable to the flow of a particular phase when it is filled only with that phase, and becomes less permeable to its flow as parts of the pore space become occupied by other fluid phases. This is illustrated in Fig. 2, where the abscissa takes into account the fact that there is an irreducible amount of water that cannot be displaced by gas, S_{iw}. The ordinate of Fig. 2 is the relative permeability, which is the ratio of the permeability of the sediment to water or gas divided by the intrinsic permeability of the sediment (the permeability of the sediment if filled only with water or gas). The figure shows pairs of curves for homogeneous sediments of decreasing permeability (grain size). The pairs of the same line type and thickness are matched, and the paired curves show how the presence of gas decreases the relative permeability of the sediment to water, and conversely. Typically, when the permeability to one phase drops, the permeability to the other rises.

The feature of Fig. 2 pertinent to the current discussion is the gap within which the permeability of fine-grained sediments is very low to *both* phases. Between about 68 and 72% reduced water saturation, the permeability to

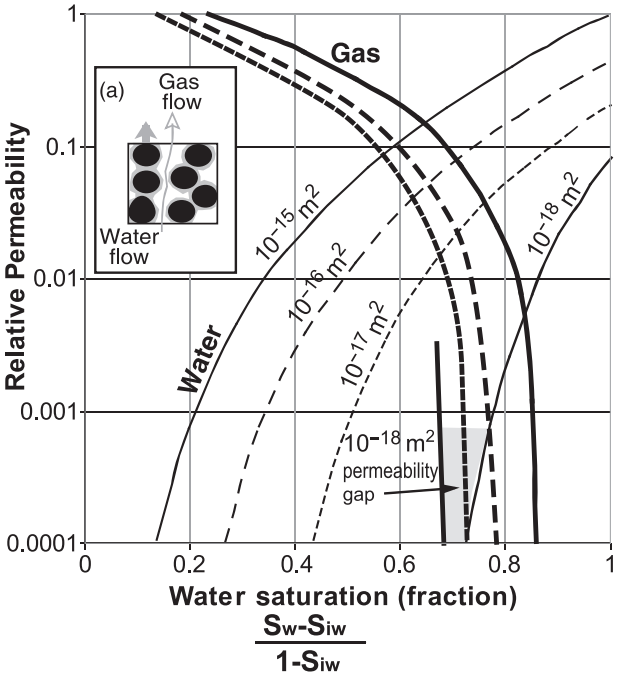

Fig. 2. Relative permeability of fine-grained sediments to the flow of water and gas when both phases are present in variable proportions in the pore space. Gas relative permeability curves are the bolder lines; water relative permeability, the lighter lines. Gas–water relative permeability pairs for the same permeability of sediment are matched by line type. Shading highlights a range of water saturation within which the permeability to both water and gas is very low in a microdarcy sediment (10^{-18} m^2). S_w is the fraction of the pore space occupied by water, S_{iw} is the irreducible water saturation. Insert (a) shows how capillary forces cause water to adhere to the solid grains and water to be pulled into the finer pores, leaving the coarser passageways for the flow of air. Figure is modified from Byrnes (2003).

both gas and water in a sediment with microdarcy (10^{-18} m^2) intrinsic permeability is reduced at least 4 orders of magnitude. The resulting 0.1 nanodarcy (0.1×10^{-21} m^2) permeability approaches levels low enough to seal over- or under-pressured gas in a basin for geologic periods of time (Deming 1994).

The ability of sediment to form seals of this kind is greatly augmented if the sediment is grain-size layered, as are all natural sediments. Conceptually what happens in this case is illustrated in Fig. 3A. Capillary forces pull water into the fine layers and the gas is rejected into the coarser layers. This is a blotter paper effect. Blotter paper pulls in ink or water and expels air to the very large air-filled 'pore' surrounding it. If a pressure gradient is imposed across a sequence of fine–coarse layers, the gas in the coarse layers will drift up against the pores of the fine downstream layer and block the flow of water through it like little toilet plungers. The gas will not be able to enter the fine pores until it is deformed to fit, and this requires a pressure drop across the fine–coarse interface. The pressure drop is easily calculated from Laplace's Law (Bear 1972; Berg 1975).

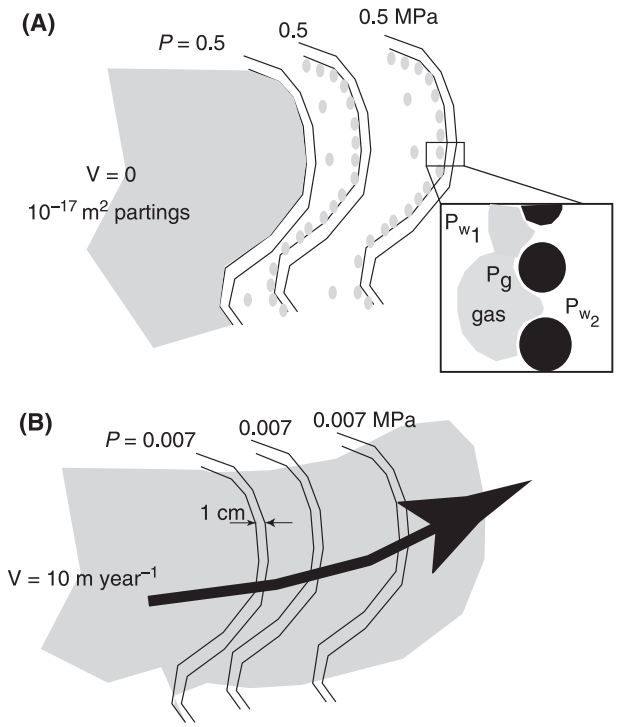

Fig. 3. (A) Illustration of how gas blocks the flow of both water and gas at fine-grained partings. As shown in the insert, surface tension, operating across the small radius of curvature of the gas in the fine pores, elevates the gas pressure of any gas bubble that partially enters the fine pores and requires that $P_{w1}-P_{w2} = \Delta P_c$. If P_{w1} does not exceed P_{w2} by ΔP_c, water will invade the small pores and push the gas out. Pressure drops of ΔP_c across a number of partings can trap overpressured (or underpressured) gas for geologic periods of time. Panel (B) shows that if a pressure increase were to cause gas to penetrate the partings they would offer little viscous resistance to flow even if the gas flux were large (see Appendix calculation 1b).

For fine-grained partings with a permeability of 10^{-17} m^2 (10 microdarcies), the gas entry pressure is about 0.5 MPa (5 atmospheres; see Appendix calculation 1a). Many fine partings conspire to produce a seal. For example, 60 fine–coarse interfaces, each supporting a 0.5 MPa pressure drop, could contain a lithostatically-pressured (70 MPa) gas accumulation at 4 km depth and block gas leakage into hydrostatically pressured (40 MPa) water-filled surroundings (see Appendix calculation 2).

Laboratory experiments are instructive. Figure 4 shows the results of an experiment (Shosa & Cathles 2001) in which fine sand layers were placed in a 1 cm ID, 50 cm long stainless steel tube filled with coarser sand. The pore space of the sediment-filled tube was filled with CO_2 gas, evacuated, water introduced, the system pressurized, and finally CO_2-charged water introduced as a single phase under pressure. This procedure assured that no gas initially occupied the pore space. Under single phase conditions (e.g. when the pressure was high enough that all the CO_2 was dissolved in the pore water), very small pressure drops developed across the 2 μm layers when flow through the tube was imposed by a piston pump, as shown in insert (a). When the pressure was lowered, so that a separate gas phase exsolved, capillary pressure drops developed at the upstream end of the fine layers that added to the pressure drops associated with flow through the fine layers (lower curve in insert). Unlike the flow-related pressure drops, these capillary pressure drops remained when the flow was stopped. The main part of Fig. 2 shows how the added capillary pressure drops developed as pressure in the tube was reduced under flowing conditions. The very small difference between pressure at the inflow and outflow ends of the tube over the initial 5 h of the experiment (when pressure was slowly lowered) indicates the small resistance to single phase flow across the five fine layers in the tube. Gas exsolved, and capillary pressure drops developed over a period of about a half hour at approximately 5.5 h. After this, the pressure decrease across the tube was the sum of the small flow resistance and the much larger 0.4 MPa/layer (4 bar/layer) capillary pressure drops at each layer. At 10 h the flow was stopped and the pressure monitored for 3 weeks. There was no measurable change in the pressure decrease across the tube over this period.

The experiments show clearly that the additional pressure drops that developed at each interface when the gas phase exsolved were *not* caused by flow interference between the two phases in the fine layers, but were rather due to capillary blockage, specifically the need to deform the gas bubbles so they could move through the pores of the fine layers. The added (capillary) pressure drops are of exactly the magnitude predicted from Laplace's Law (Berg 1975). This Law states that the capillary pressure drop across the layers equals the product of the gas–water interfacial tension and the difference in the inverse of the radii of the fine and coarse pores (e.g. assuming a wetting angle close to 0°, $\Delta P_c = 2\gamma(1/r_{fine} - 1/r_{coarse})$, where ΔP_c is the capillary pressure drop, γ is the interfacial tension between gas and water, r_{fine} is the radius of the fine pores, and r_{coarse} is the radius of the coarse pores). Laplace's Law contains neither permeability nor viscosity as variables. The magnitude of the capillary pressure drops (the pressure change across the tube under no-flow conditions) changed with temperature in proportion to the change in the gas–water interfacial tension with temperature, which is very different from the change in water or gas viscosity with temperature. The additional flow resistance is thus not caused by relative permeability interferences in the fine layers but by capillary *blockage*. The distinction is important because, for capillary blockage, there can be no flow unless the pressure drop needed to deform the gas bubbles sufficiently to enter the fine pores at a fine–coarse interface is exceeded. Once this pressure drop is exceeded, flow can occur and the flow will obey the relative-permeability relations. Before the gas entry pressure is exceeded, the only

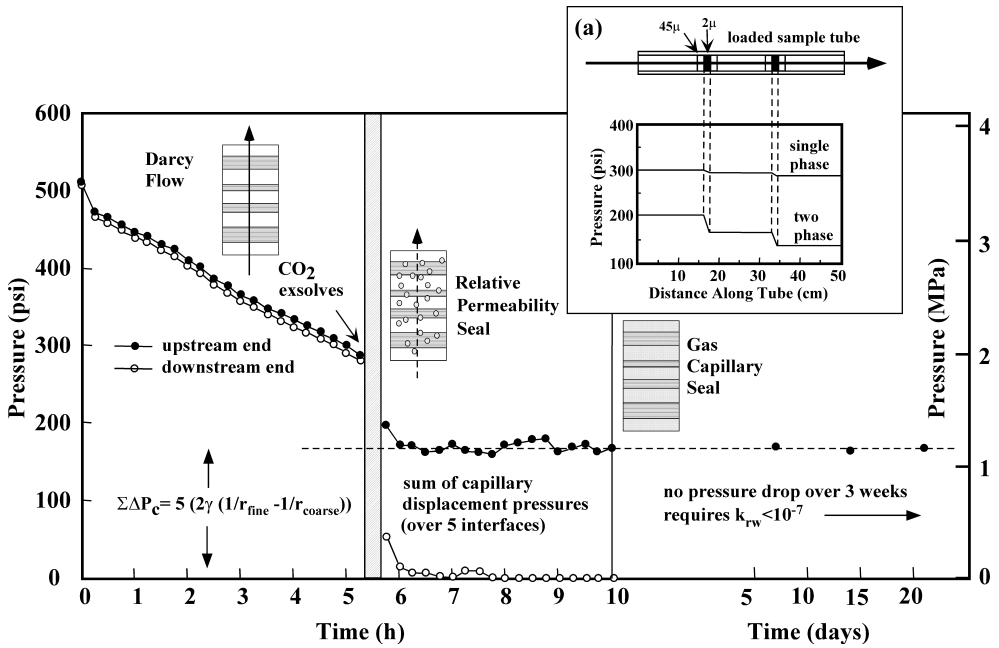

Fig. 4. Experiment illustrating capillary blockage at fine layers. Layers of fine grained quartz were placed in a 1 cm ID tube and CO_2-rich water introduced as a single phase. Insert (a) schematically shows pressure drops across the fine layers under flowing single- (upper line) and two-phase (lower line) conditions. The main figure shows the changes in pressure drop across the tube that occurred as total pressure was lowered, gas exsolved, and two-phase flow began. Under single-phase flow conditions (<5.4 h) the pressure difference between the upstream and downstream ends of the tube is very small. When CO_2 exsolves (approximately 5.5 h) the pressure drop becomes large. Flow was stopped at 10 h. There was no measurable change in the pressure difference over the following 21 days. The two-phase pressure drop equals the sum of the calculated capillary pressure drops across the five fine layers in the tube. Symbols are defined in the text. Figure is composite of the figures in Shosa & Cathles (2001).

water flow possible is around the edges of the gas bubble that is pressed tightly against a pore. But this gap is so narrow that the water is an ordered structure and behaves like immobile ice. This is shown by the extremely low relative permeability (10^{-7}) calculated from the lack pressure change across the tube over the 3-week period at the end of the experiment (Fig. 4). Full details of the experiment are given in Shosa & Cathles (2001). Related papers in the same publication describe the broad implications of capillary seals in basins (Cathles 2001), their implications for porosity-depth profiles in basins (Revil & Cathles 2001), and their potential impact on oil production under conditions of gas exsolution (Erendi & Cathles 2001).

Capillary seals are good candidates for preserving over- or under-pressured gas in basins for hundreds of millions of years because they block rather than impede the flow of both phases. But they are good seals for perhaps an even more important reason: they can re-heal after rupture. Over hundreds of millions of years, any basin is likely to be deformed and fractured many times. Capillary seals are uniquely able to re-heal themselves because, after any fracturing, the ingredients of sealing (two phases and a grain size contrast) are still present. After a slight loss of fluid during the fracturing event itself, the seal will re-establish itself and be as effective as before.

The operation of a gas pulsar

With this background we can understand how the nonlinear characteristics of capillary seals might allow them to repeatedly and rapidly release large volumes of gas. Consider a basin-centered gas zone such as that in the Arkoma Basin, which abuts a brine-filled aquifer near its top (Fig. 5A). Suppose the gas pressure in the gas zone is such that the pressure is above hydrostatic near its top, where it contacts the aquifer, but that capillary seals associated with shale partings or fault gauge layers between the gas zone and the water-saturated aquifer prevent the escape of gas into the aquifer as illustrated in Fig. 5B(A).

Now suppose that the pressure in the gas zone is increased for some reason. The increased gas pressure might cause the capillary seal separating the gas zone and the aquifer to begin to leak, and gas to move through, and displace water from, the closest shale partings, as shown in Fig. 5B(B). As soon as the gas displaces water from the first coarse layer and penetrates the first parting, the capillary pressure drop at this parting vanishes, and the entire overpressure is transferred to the remaining partings. The next parting is more vulnerable to gas penetration than before, and when it fails the remaining partings are still more vulnerable. In this fashion each

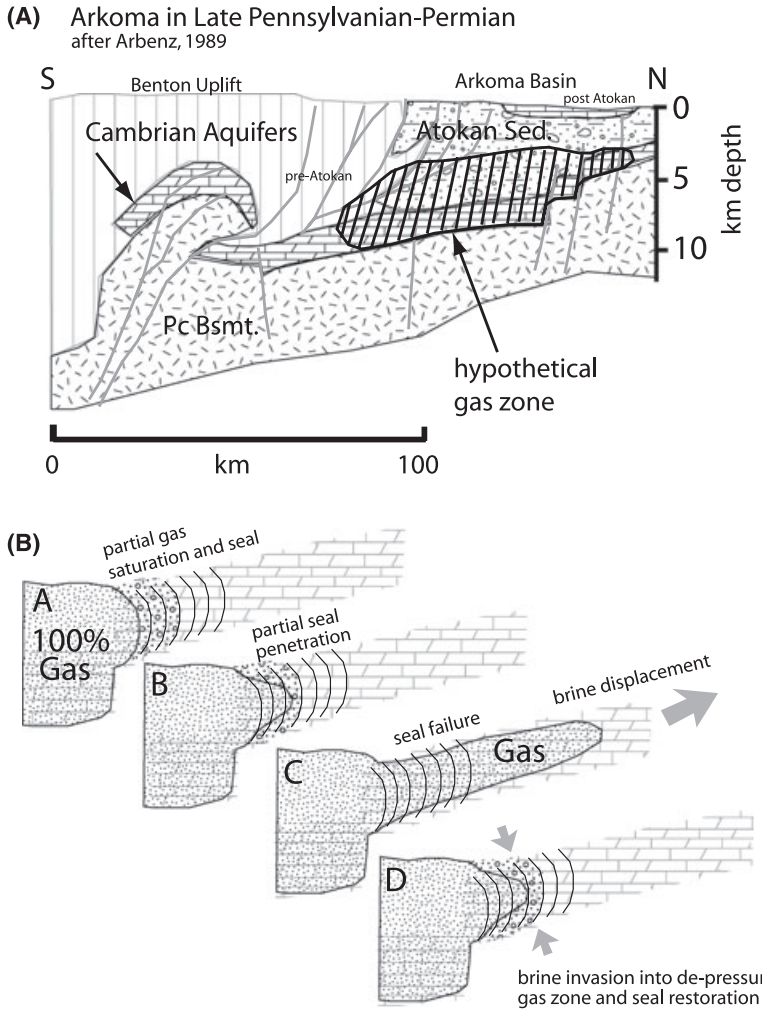

Fig. 5. (A) The Arkoma Basin in Late Pennsylvanian–Permian time with a hypothetical gas zone. Base figure is from Arbenz (1989). (B) Illustration of the operation of a gas pulsar discharging into the Cambrian aquifers at the north side of the Arkoma. In (A) the Arkoma gas is contained in an overpressured condition by capillary seals in the partial gas saturation zone that separates the gas zone in the basin from the adjacent aquifer brines. In (B) a pressure increase in the Arkoma gas zone has caused gas to penetrate through some of the fine-grained capillary barriers (shale partings or fault gauge) of the seal, compromising the ability of the seal to retain the pressurized gas in the Arkoma. In (C) the seal has fully failed and a pulse of gas has been rapidly injected into the permeable Cambrian aquifers. In (D) water has infiltrated the margins of the now decompressed gas zone and the capillary seal is in the process of reforming.

successive parting could be penetrated by gas with the result that the seal is rapidly breached (Fig. 5B(C)). A potentially large volume of gas could be released into the aquifer because, once penetrated, the partings will offer very little resistance to the flow of gas. As is shown in Fig. 3B, the pressure drop across each parting would be very small compared to the capillary barrier pressure drops when the seal was intact, just as in the experiment shown in Fig. 4. The pressure drops are calculated in Appendix calculation 1b.

The release of gas would cease when the gas zone depressured sufficiently. At this point, water could move into the areas from which it had been displaced, be drawn into the fine shale partings, and the seal would re-heal as shown in Fig. 5B(D). If the gas zone pressure increased again, the seal might fail again, and another pulse of gas would be released into the aquifer. In other words the basin-centered gas zone could act as a gas pulsar, repeatedly delivering pulses of gas into a permeable brine-filled aquifer that abutted it.

The enigmatic nature of MVT deposits

The preceding discussion describes a mechanism for delivering pulses of gas into an aquifer. MVT lead–zinc deposits are associated with basins with basin-centered gas, and require episodic and rapid pulses of brine expulsion. The summary below elaborates on these statements. It is condensed from a more extensive review by Cathles & Adams (2005) which summarizes the characteristics of MVT deposits in more detail and critically evaluates the various mechanisms that have been proposed for their formation. The reader is referred to this reference for additional discussion.

Lead–zinc mineralization is easily produced. Only two ingredients seem to be necessary: a very saline brine with $>10^5$ ppm chlorinity (Hanor 1997) and the expulsion of that brine to the surface. The ubiquitous distribution of sub-economic lead–zinc mineralization around basins containing suitably saline brines is striking. Basins seem to have deposited base metals whenever brine was expelled (Cathles & Adams 2005).

Mississippi Valley-type deposits typically form when brine is expelled along a particularly permeable basal aquifer. The deposits tend to form hundreds of kilometers from the source basin within a kilometer of the surface, either in the aquifer itself or in permeable structures (faults or karstic reefs) that connect to it. These deposits are remarkable because they were *briefly hot* at the time of their formation. Apart from this they would be as easy to form as other types of lead–zinc mineralization and, as they are in such logical brine escape structures, they would be considered well understood. Their brief heating requires pulses of rapid brine expulsion. Pulses of mineralization suggest such pulses of fluid flow. In the Buick Mine in the Viburnum Trend, eight pulses of mineralization have been noted (Sverjenski 1981). In the Tri-state district, eight intervals of chalcopyrite deposition, six intervals of sphalerite deposition, and five intervals of galena and quartz deposition have been documented (Hagni 1976). MVT deposits seem to have formed only since the latest Proterozoic. The oldest known MVT deposit is the Nanisivik deposit in the Canadian Arctic, paleomagnetically dated at 1095 Ma (Leach *et al.* 2001). Glacial periods seem to have been particularly productive of MVT deposits.

Figure 6 summarizes the evidence for brief heating of the sites of MVT ore deposition. It is based on a summary by Sangster *et al.* (1994). The deposits are shown as crossed hammers at the depths at which they are considered to have formed. The range of fluid inclusion homogenization temperatures measured in gangue minerals associated with the ore is indicated above each crossed hammer symbol. Below each deposit, a circle with error bars indicates the depth from which brines would need to have been derived to be as hot as indicated by the fluid inclusion data, assuming a geothermal gradient of 20°C km^{-1} and a surface temperature of 15°C. The conodont alteration index (CAI) found in strata in or very near each deposit is given above each of these symbols. The maximum time interval that the deposit could have been at the fluid inclusion homogenization temperatures and not mature the conodonts more than observed is indicated below the CAI indices. The figure shows that: (1) the deposits plotted were all anomalously hot at the time of ore deposition (the circles with error bars all lie at depths much greater than the depths at which the deposits formed), (2) the source depth of the brines that deposited ore was at least approximately 4.5 km, and (3) the deposits were at their ore deposition temperatures for at most 100 000–200 000 years (because if they there were hot longer than this their CAI indices would be greater than observed). Other data support the conclusion that the heating was brief.

Almost all the MVT deposits in North America are associated with basins with basin-centered gas (Cathles & Adams 2005). The Pine Point MVT deposit in the North

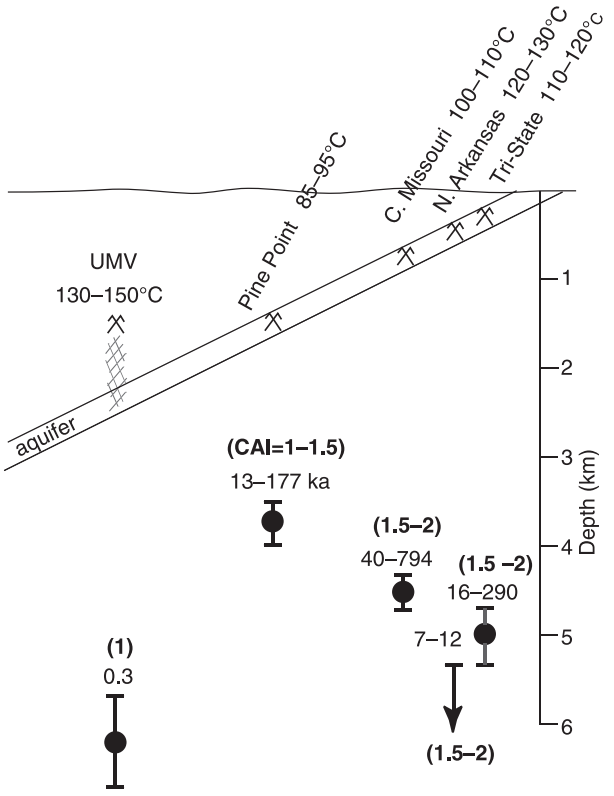

Fig. 6. Depth of formation of MVT deposits for which fluid inclusion homogenization temperatures and conodont alteration index (CAI) maturity measurements are available (from Sangster *et al.* 1994). Crossed hammers show the depth of the deposits at the time of ore deposition. The range of fluid inclusion homogenization temperatures showing the temperature at the time of ore deposition are shown above the deposit symbols. The deposits are either within a permeable basal aquifer or in a permeable connection to it, as illustrated. Data points underlying each deposit show the depth from which brines must have originated to have the fluid inclusion homogenization temperatures in the deposits, assuming a surface temperature of 15°C and a temperature gradient of 20°C km^{-1}. CAI maturity indices measured at the deposits are shown in parentheses above each data point, and the period of time the site could be heated to the fluid inclusion homogenization temperatures and not matured more than indicated by the CAI indices is indicated below these numbers. Methods of calculation are discussed in Cathles & Adams (2005).

West Territories is associated with the WCSB where basin-centered gas was first produced and documented, and the MVT deposits in the mid-continent of the US are associated with either the gas-filled Arkoma Basin or the Appalachian basin which has extensive basin-centered gas. Basins with overpressured brine, such as the Anadarko Basin, which is adjacent and otherwise similar to the Arkoma, do not have associated MVT mineralization. Many MVT deposits contain hydrocarbons. Sphalerite at the Cadjebut deposit is purple because it contains so many hydrocarbon-filled inclusions (Eisenlohr *et al.* 1994), for example.

Figure 7 shows the MVT deposits associated with the Arkoma Basin and the basal aquifer system through which

brines are thought to have moved from the Arkoma Basin to the sites of ore deposition. The flow pattern of the brines is suggested by the reduction of hematitic pigments in Missouri (Goldhaber *et al.* 1995) and by the northward decrease of authogenic fluorine picked up from intrusions near Hicks Dome (Rowan & Goldhaber 1995). If current perceptions are correct, the brines that formed the MVT deposits in the Central Missouri, Tri-State, Viburnum Trend, the Old Lead Belt, and the Upper Mississippi Valley district deposits came from the Arkoma Basin as suggested by the black arrows in Fig. 7.

Could a gas pulsar be responsible for MVT ore deposition in the mid-continent of North America?

As shown in Figs 5a and 7, basin-centered gas in the Arkoma contacts the very permeable basal Cambrian sandstone (Lamotte and Mt Simon) and karstified carbonate aquifers of the North American mid-continent. These Cambrian aquifers connect to the sites of MVT ore deposition. Could a gas pulsar, operating in the Arkoma in the manner shown in Fig. 5, have injected gas into these aquifers rapidly enough and in large enough volumes to displace the

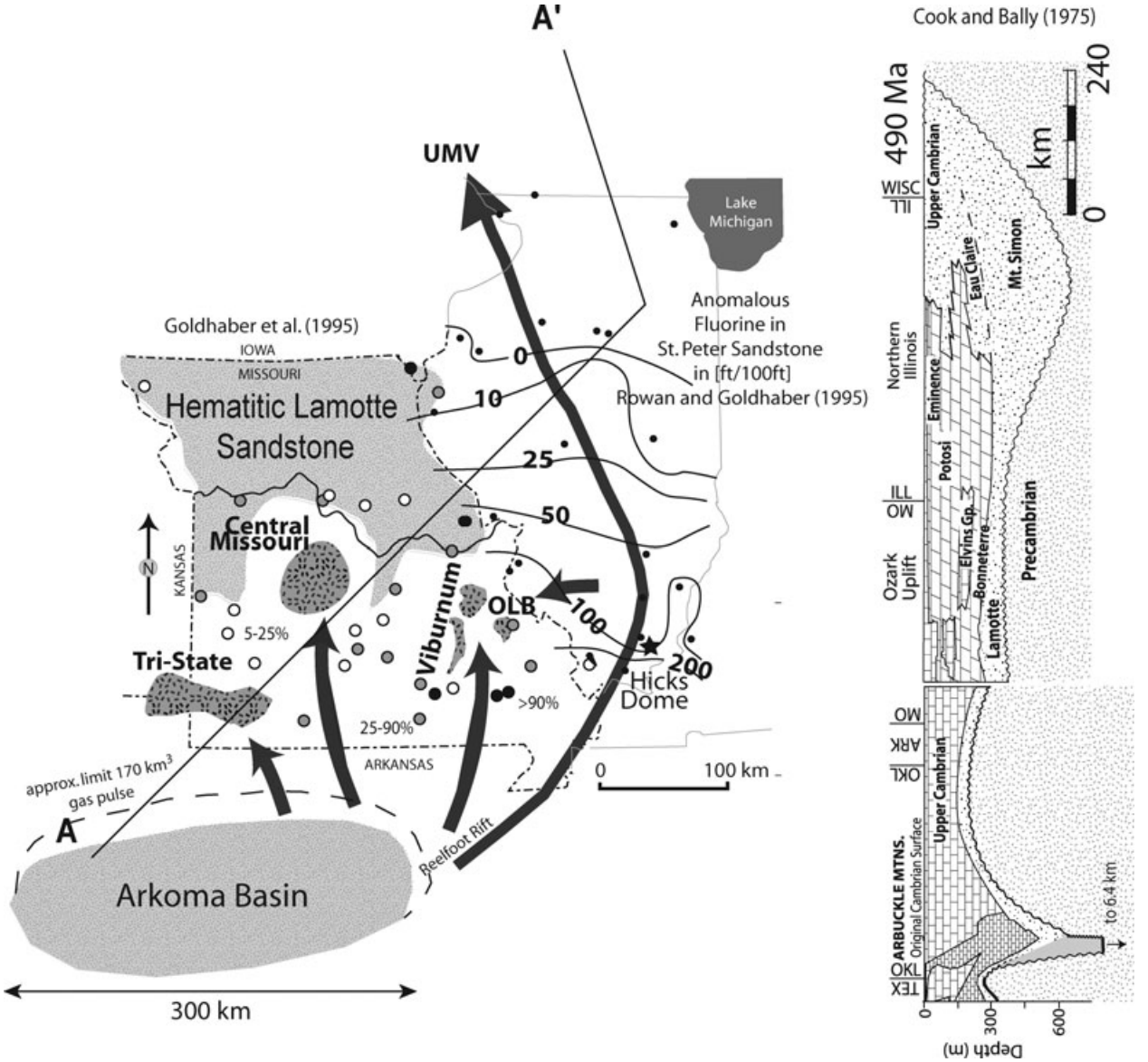

Fig. 7. Possible flow paths from the Arkoma Basin to MVT districts associated with it. Brine flow occurred through the extraordinarily permeable Cambrian sandstone and karstified limestone aquifers shown in the section to the right. Patchy reduction of hematitic pigments of the Lamotte sandstone and the decreasing fluorine content of the Lamotte toward the north suggest the northward flow of brines (Goldhaber *et al.* 1995; Rowan & Goldhaber 1995). Flow tubes through these aquifers that might have operated during one pulse of expulsion are shows as arrows. Section AA′ is a composite from Cook & Bally (1975). Figure is a modified combination of Figures 4, 23, 24 in Cathles & Adams (2005).

brine needed to perturbed temperatures and deposit base metals at the sites of MVT ore deposition in the fashion observed? Under restrictive conditions, the answer to this question appears to be yes.

Gas volumes in the Arkoma

The Arkoma Basin today has average dimensions of approximately $300 \times 100 \times 10$ km and is substantially filled with gas. At an average porosity of 5%, it would contain 15 000 km^3 of gas. If the gas at the top of the gas zone was at 4 km depth and was initially close to lithostatic pressure, decompression to hydrostatic conditions would increase the gas volume in the basin by approximately 136% and approximately 3240 km^3 of gas would be expelled into the mid-continent aquifer system (see Appendix calculation 3). Additional gas might be contributed by ongoing maturation as discussed below.

The volume of brine displaced by the introduction of even 3000 km^3 into the aquifer system is much more than is needed to supply the metals for the associated MVT mineralization. More than 100 ppm combined lead plus zinc is found in brines with chlorinities greater than 10^5 ppm (Hanor 1997). Thus approximately 570 km^3 of brine could supply the 57 billion tones of base metal found in all the deposits associated with the Arkoma Basin (74% of which is in the Viburnum Trend, 14% in the Old Lead Belt and 10% in the UMV deposits). Three thousand cubic kilometers of displaced brine is >5 times that needed for the economic mineralization. It is enough to account for dispersed (sub-economic) mineralization and accommodate low efficiencies of ore deposition. The more difficult question is whether brine expulsion could be rapid and voluminous enough along the flow paths to the MVT deposits to transfer the heat from the deeper parts of the basin to the sites of ore deposition.

Brine volumes required for heating

It would be difficult to heat pathways from the Arkoma to the MVT deposits in the absence of substantial channeling of brine flow. From Fig. 7, for example, the plan area between the Arkoma and the Missouri mineralization is approximately 75 000 km^2. As the heat capacity of brine is about twice that of brine-saturated rock, a 1 km-thick portion of the basal aquifer underlying this area can be heated by the uniform (i.e. largely unfocussed) expulsion of approximately 37 500 km^3 of brine. This is substantially more than the 3000 km^3 that is easily available. If the flow was channeled, the volumes could be much less, however. For example, a 1 km diameter tube 250 km long has a volume of 186 km^3 and would require only 93 km^3 of brine to heat.

The volumes and flow rates needed to deliver hot brines to the sites of MVT mineralization can be estimated more accurately using a dimensionless vent number that characterizes the heating of cylindrical flow tubes similar to those just described (see Table A1). This vent number is the ratio of the heat introduced into the cylindrical flow tube to the heat lost from the sides of the tube if it was at input temperature for the period of heat introduction. The flow tube is assumed to be in an environment in which the unperturbed temperature decreases linearly from the entry to the discharge end. The vent number is a function of the time that brine has been flowing through the tube as well as the rate of flow through the tube and the width and length of the tube. If the vent number, N_v, is <0.1 the brine in the tube has nearly the same temperature as its surroundings. If $N_v \sim 2$, the tube is warmed to entry temperature along its entire length, and hot brine can be delivered to the sites of MVT mineral deposition. The dimensionless vent number is discussed and documented in Cathles *et al.* (2006).

Figure 8 shows the durations and total volumes of venting required to produce $N_v = 2$ in flow tubes 250 km long with diameters between 50 and 1000 m. The throughput of brine required to warm the flow tubes is less for shorter venting times because less surrounding sediment is heated. Smaller diameter flow tubes require less brine to heat. Figure 8 shows that a 50 m diameter flow tube 250 km long can be heated to input temperature by the throughput of approximately 60 km^3 of brine over a period of 5000 years.

Gas delivery

By hypothesis, the brine is driven through the flow tubes when gas rapidly enters the aquifer after the capillary seals retaining the gas in a basin fail. As shown in Appendix calculation 4, if the basin-centered gas zone has 2.5 microdarcy permeability, 5000 years after seal failure decompression will extend approximately 10.4 km into the basin-centered gas zone. On average, 18% of the contained gas will be expelled from the decompressed volume. If the porosity of the approximately $300 \times 10.4 \times 6$ km volume is 5%, approximately 170 km^3 of gas will be expelled. When it enters the 300 m-thick Cambrian aquifers, this gas will extend approximately 18 km from the edge of the Arkoma, assuming the aquifers have a 10% porosity and that the gas penetration is uniform (see Fig. 7). In fact, the penetration is likely to be irregular, with gas extending much further in some areas. Once the gas enters the very permeable Cambrian aquifer system it will quickly buoyantly rise to the uppermost parts of the aquifer. Lacking durable traps in the overlying stratigraphy, the gas will leak through the overburden and eventually vent into the atmosphere. As it rises and decompresses it will expand and

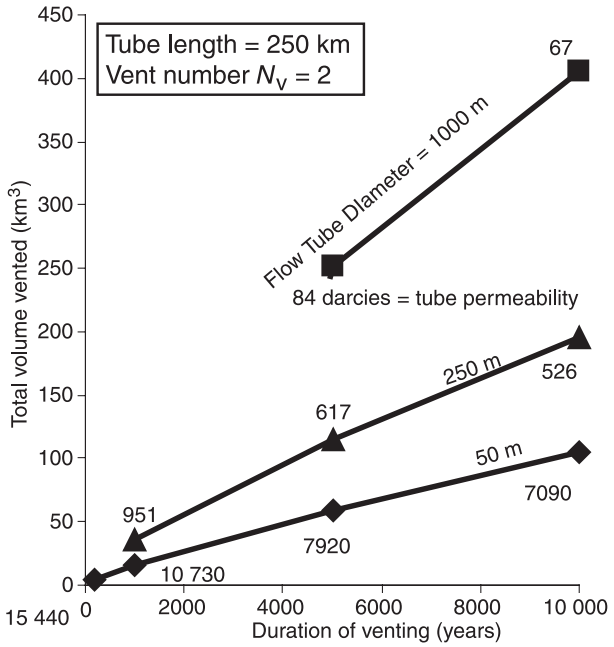

Fig. 8. The combinations of brine volume and the duration of venting required to deliver hot brine through cylindrical flow tubes of different diameter are indicated by lines. The tubes are all 250 km long and fully heated at the end of the time interval of venting (vent number $N_v = 2$). The permeability required for brine to vent through each tube at the rate specified is given in darcies (10^{-12} m^2) above each data point, assuming the pressure at one end of the tube is 30 and 0.1 MPa (atmospheric) at the other. The volumes injected (left axis) introduced many times the heat required to warm the tubes. For the 50 m diameter tube the amount of heat injected is 16 (200 years venting) to 365 (10 000 years venting) times that needed to heat the 250 km long tube. The methods of vent number analysis are given in Cathles *et al.* 2006.

drive additional brine along the most permeable escape pathways of the Cambrian aquifer system.

Brine delivery

As soon as gas enters the Cambrian aquifers it will displace an equal volume of brine. If the brine relatively quickly moves into particularly permeable flow tubes that are approximately 50 m in diameter, three tubes could deliver heat to deposit sites 250 km distant (e.g. three tubes would transmit approximately 60 km^3 of brine each over the 5000 expulsion period).

Suppose that after 5000 years the boundary zone between the Cambrian aquifers and the Arkoma gas had depressurized sufficiently for water to move back into the areas of the seal that had been invaded by gas and re-heal the seal. If gas pressures recover, the seal could fail again. If the basin ultimately looses approximately 3000 km^3 of gas, 17 pulses of brine, each 170 km^3 in volume, could be discharged. If gas generation replenished the volume lost, twice this number of pulses could be delivered. Many pulses of hot brine delivered to the sites of MVT ore deposition could precipitate the base metals that form them. If a deposit received 10 pulses of brine and was hot for 2500 years during each pulse, the deposit would be hot for approximately 25 000 years, which is well within the conodont maturation limits for most of the deposits shown in Fig. 6. Fewer pulses of mineralization and faster venting for less time could deposit the ore within a shorter period of heating.

The brine would undoubtedly enter flow tubes of irregular cross sections with a range of dimensions. At least one particularly permeable tube must connect to the UMV district. The situation will be much more complex than sketched above. The intention in this paper, however, is only to describe how the system might operate – to show that the system could operate in a way that allows hot brines to be delivered to all of the mid-continent MVT deposits associated with the Arcoma Basin in a fashion that is compatible with the thermal constraints and the other observed aspects of these deposits.

Reloading the pulsar

About 310 Ma ago over 5 km of sediments accumulated very rapidly in the Arkoma Basin. This is illustrated in Fig. 9, which also shows that, according to paleomagnetic dating, the mid-continent MVT deposits continued to form up to 60 Ma *after* sedimentation in the Arkoma ceased and the Ouachita accretionary prism had stopped growing. The active hydrocarbon generation that may be important to re-pressurizing a gas basin is expected to continue for approximately 60 Ma after sedimentation ceases, however. The reason is that the approximately 5.5 km of rapid sedimentation that occurred in the Arkoma with the deposition of the Atokan sediments depressed the isotherms in the crust and lithosphere, and it took approximately 60 Ma for them to thermally recover. Over this period, heat flow to the basin increases and the sediments warm (Hutchinson 1985). This phenomenon can be seen in the Gulf of Mexico, where present-day sedimentation rates almost as rapid as occurred in the Arkoma currently depress heat flow by a factor of 2 compared to areas where sedimentation ceased 60 Ma ago that have had time to thermally recover (Cathles & Losh 2002, see also Cathles & Adams 2005). Thus, the depth to the top of the gas generation window in the Arkoma was likely decreased by a factor of 2 in the 60 Ma that followed the cessation of rapid sediment deposition. The time required to generate 170 km^3 of gas depends on the organic richness of the strata being passed by the top of the gas window. At 1% total organic carbon, which is a low value for organic shales or carbonates, the time required is approximately 10 Ma; at 2% total organic carbon (TOC), 5 Ma would have been required (see Appendix calculation 5). Thus, depressurized gas volumes in the Arkoma could have

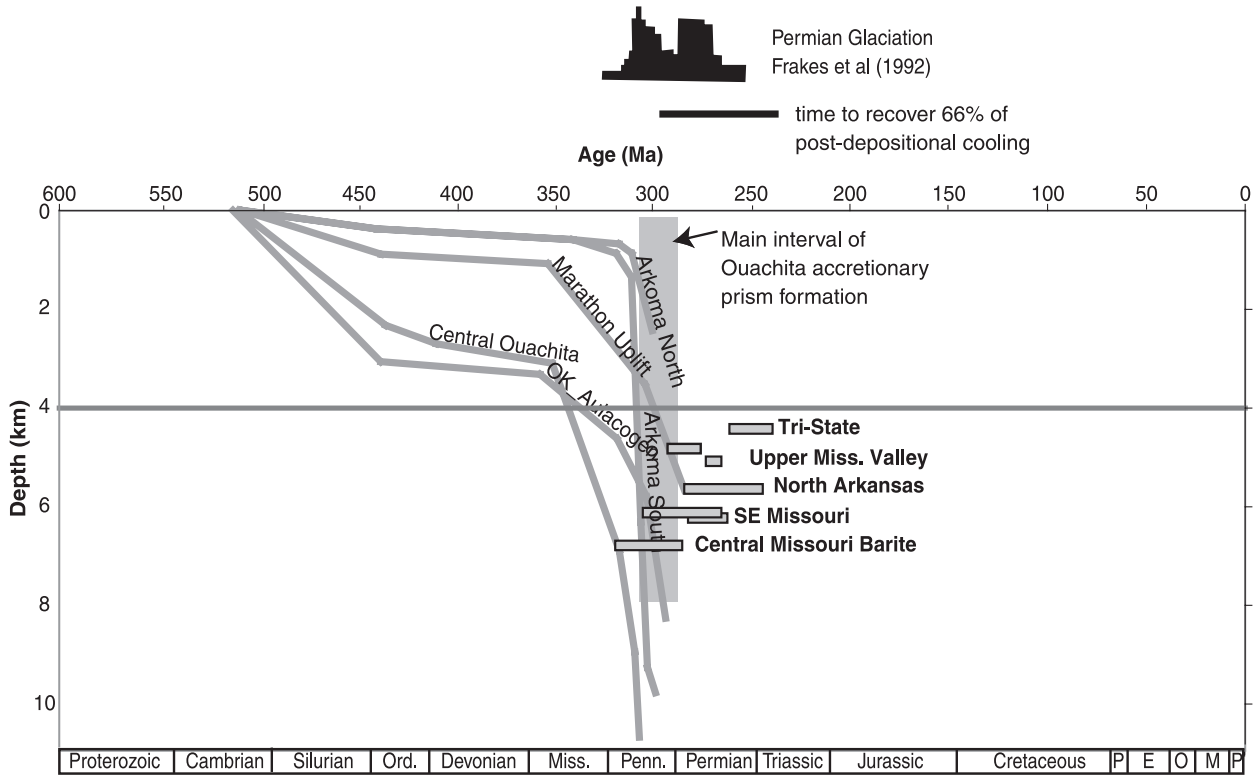

Fig. 9. Subsidence curves for the Arkoma and adjacent foreland basins, the main interval of formation of the Ouichita accretionary prism, the time span of Permian glaciations as indicated by age dates on glacial and ice rafted deposits from Frakes *et al.* (1992), and the time span (bar at top) over which the Arkoma sediments will recover 66% of the temperature depression caused by the rapid deposition of 5.5 km of Atokan sediments are shown relative to the paleomagnetic formation ages for MVT deposits associated with the Arkoma basin (from Leach *et al.* 2001). References for the subsidence curves are given in Fig. 2 in Cathles & Adams (2005). This figure is a simplified version of that figure.

reloaded several times in the post-sedimentation period when the MVT deposits formed.

A trigger for the gas pulsar

A final first-order question involves the circumstances under which the capillary seals trapping gas in a basin can fail catastrophically. Gas pressures greater than about 0.8 times lithostatic cannot be retained because pressures greater than this will hydrofracture the sediments. The seal may leak at pressures less than this, however, depending on the number of partings or gauge layers available. If maturation reactions raised pressures in a basin such that the seal starts to leak, slow leakage could control further increases in pressure. In other words, the seals might leak slowly as gas was generated. To get large volumes of gas introduced suddenly into an aquifer system we need a general failure of the capillary seals that separate the gas zones of the basin from the aquifer, and loss of pressure in an appreciable volume of the gas zone after this general failure. What could trigger this kind of general failure?

As discussed earlier, the key to rapid and complete seal failure is the penetration of gas through a few of the partings that comprise the seal (Fig. 3B). The penetration must be such as to trigger a cascade of parting penetrations that is rapid enough to displace the water from a relatively large volume of the seal. Otherwise water will be available to heal each parting, and the seal will only leak as needed to keep the pressure drop across it at a relatively constant level.

Anything that rapidly increases the gas pressure at the top seal could trigger a general seal failure. The rise in sea level that occurs when major continental glaciers melt is one of the most rapid loading mechanisms in the natural world. A 100 m rise in sea level in 5000 years is equivalent to a sedimentation rate of 9 km Myr^{-1}, for example. The maximum sediment deposition rates in places like the Gulf of Mexico are approximately 2 km Ma^{-1}. Sedimentation as rapid as 9 km Myr^{-1} is probably achievable only during evaporite deposition. If a portion of the gas-filled part of a basin is overlain by ocean where it would be subject to this meltwater loading, the gas pressure in this area would increase by nearly the full amount of this applied load (Appendix calculation 6). If there is a relatively permeable network in the gas zone connecting its loaded parts to the seals in contact with the aquifer, the increased gas

pressures in the loaded zone could be transmitted to the area where the gas zone abuts a permeable aquifer, and this could trigger seal failure and the rapid release of a large volume of gas into the aquifer. For example, for 10 microdarcy partings, the capillary pressure drop across each parting is 0.5 MPa. If the pressure drop across each partings is close to this maximum (as would be the case in a basin generating gas and constantly on the verge of leaking), the increase in pressure required to cause leakage will be much less than 0.5 MPa, and an increase in the gas pressure of 1 MPa (100 m meltwater) load could cause gas penetration through a great many partings and trigger the general failure of the capillary seals. Under favorable conditions (see quantitative discussion in Appendix calculation 6), the rapid sea level rise associated with melting continental glaciers could be a good way to trigger the sudden release of large volumes of gas from an overpressured gas-filled basin. A meltwater rise in sea level is certainly not the only way a gas pulsar event might be triggered, but it is an interesting way.

The flow tubes must be very permeable

Cathles & Adams (2005) argued that loading *underpressured* gas zones in the Arkoma by 100 m of glacial meltwater could expel the gas volumes needed for MVT mineralization. Although possible, this now seems, for two reasons, not to be as viable a mechanism for MVT formation as the one proposed above: First, it is much more difficult to preserve uncompacted porosity in an underpressured gas-filled basin than in an over-pressured one. Excess (uncompacted) porosity can persist to approximately 8 km depth in an overpressured basin but only to approximately 3.5 km depth in a normally pressured basin (Cathles & Adams 2005, Appendix 2). If the top of the gas zone is at 4 km depth, there will not be much gas in this fully compacted part of the basin. Second, the overpressures are useful in driving brine flow at the rates required.

The numbers above each calculated data point in Fig. 8 show the permeability required for each flow tube to deliver the indicated volume of brine across 250 km in the indicated time, assuming the excess pressure (e.g. the pressure in excess of hydrostatic) at the entry end is 30 MPa. This is the excess pressure the gas would have if the top of the gas zone were at 4 km depth and at 0.8 of lithostatic pressure (see Appendix calculation 2). As shown in Fig. 8, the flow tube permeabilities required are generally $\sim$1000 darcies (10^9 m^2) and sometimes considerably more. The flow tubes must therefore be karstic carbonates or gravels (sediments with grain size greater than 2 mm). Flow paths this permeable through the very mature Cambrian sands and karst connections in the Cambrian carbonates are certainly possible, but are nevertheless challenging. If the Arkoma were underpressured, the driving pressure would be approximately 1 MPa (the meltwater load) and the permeabilities would need to be 30 times greater. Finding pathways this much more permeable could be even more challenging.

SUMMARY AND DISCUSSION

This paper presents arguments that a fundamental change in sub-water table flow occurred at the end of the Proterozoic when organic matter began to be buried in sufficient quantities that a substantial fraction of the sub-water table pore space could be occupied by gas. From this time, gas could be generated and trapped in large portions of basins for geologic periods of time. Under certain circumstances the basin-centered gas accumulations could operate as gas pulsars and rapidly expel portions of their contained gas into adjacent permeable, brine-saturated, aquifers. This paper shows that the gas ejections could have displaced aquifer brines rapidly enough, and in sufficient volumes, to form MVT lead–zinc deposits, a type of ore deposit known only in post-Proterozoic time.

Basin-centered gas has been known for some time, but it has only recently been suggested that basins containing basin-centered gas could be related to MVT deposits (Cathles & Adams 2005). The gas pulsar mechanism for MVT formation proposed here is entirely new. Its most attractive aspect is that it can explain in a very natural fashion all the enigmatic aspects of MVT deposits. The hypothesis explains why MVT deposits are restricted to post-Proterozoic time, provides a way to assure brines are not diluted (pure displacement), which would compromise their ability to transport base metals, explains the episodic and varied nature of ore deposition (multiple brine pulses of various volume from different parts of the basin delivered along different pathways to the same vent/deposit locations), explains how the deposits can be heated for only a cumulatively short period of time, and explains why glacial periods may favor their formation. Finding even one physically plausible mechanism compatible with these observations has proven to be difficult.

Operation of a gas pulsar in a fashion that could form MVT deposits can happen only under a quite restrictive set of conditions. The gas-filled portion of the basin must have a bulk permeability approximately 2.5 microdarcies or greater to release the required volumes of gas quickly enough, the contact between the gas zone and the basal aquifers must be long and under sufficient cover that the temperature is $\gtrsim$120°C, there must be very high permeability, low-volume channels through the aquifers, and these channels must connect to the surface/deposit sites far enough from the contact that pulses of brine, and not gas, are delivered through them. The rapid rise in sea level that occurs when continental glaciers melt provides a good trig-

ger for a gas pulsar if the permeability structure of the gas zone is such that the pressure increase in loaded areas can be transmitted to the areas where the gas zone contacts a very permeable aquifer.

Operation of a gas pulsar is examined in the context of the MVT deposits associated with the Arkoma Basin. Only one of potentially many scenarios of operation is presented. Only the pulsed expulsion of gas *after* sedimentation has ceased is described, although gas could have been expelled during sediment accumulation, when the basin filled initially with gas, or during the compression that formed the Ouachita accretionary prism. Pulsed expulsion of gas might have occurred at these times if the conditions were right, and, although this seems not to have been the case for the Mid-continent deposits we discuss, these scenarios may be relevant to other MVT deposits. There are undoubtedly many ways that the highly nonlinear discharge of gas from a gas zone in a basin might occur. Portions of a basin may separately decompress. A special trigger for these events may not be necessary. They might decompress sequentially, like a line of dominos. I do not mean to discard many other possibilities or scenarios by discussing only melt water loading.

Analysis of the single scenario is approximate. All parameters could be easily changed by a factor of 2 or more. Simplifying assumptions have been made everywhere. For example, it is assumed in the vent number analysis that the unperturbed host temperature decreases linearly along a flow tube from the gas zone margin to the vent/deposit. This effectively assumes the channel rises toward the surface with a constant slope, which is certainly not the case. In many cases, only the time average of a quantity is considered. For example, the restrictions of gas zone permeability are explored using the average venting rate over 5000 years, and constraints at early times of venting or for shorter periods of venting are not discussed. These considerations will become important if detailed models of the process described here are constructed. The simplifications and approximations do not affect conclusions regarding the plausibility of the gas pulsar mechanism, which is the concern of this paper.

Several aspects of the gas pulsar phenomenon remain unclear. For example, it is not obvious how a basin that partially decompresses will ultimately fully decompress. The observations summarized by Law (2002) suggest basins can partially decompress because portions of some gas-filled basins are overpressured whereas other portions of the same basin are under-pressured. Basins that do, eventually, fully decompress may have the kind of internal structure needed to make a melt water trigger viable. Water-rich zones within a basin-centered gas zone could form interior capillary seals and make pulsar discharge more complex. We have a lot yet to learn about the nonlinear operation of gas zones, and this is a major point of this paper.

An advantage of the gas pulsar hypothesis is that it makes a large number of very specific and testable predictions. Channels of 100 to >1000 darcy permeability must connect the Arkoma the mid-continent MVT deposits associated with it. These channels must be of restricted volume. If no other plausible mechanism for rapidly propelling large volumes of brine through such channels can be found, all MVT deposits should be associated with basin-centered gas. If melt water loading is an important trigger, most MVT deposits should form during glacial periods, and at least parts of the gas zones of the basin that produced them must be overlain by ocean. Their gas zone must have an internal network of millidarcy permeability.

In the short term perhaps the most important test of the gas pulsar hypothesis of MVT formation may come from its impact on exploration. MVT deposits should be associated with under-pressured basin-centered gas accumulations of substantial magnitude that are permeable enough to be relatively easily produced. A permeable network within them could be useful in extracting gas from these basins. Very permeable aquifers must contact the upper parts of the gas zone to MVT deposits. The upper parts must be relatively deep (approximately 4 km). MVT deposits should form particularly at times of continental glaciation. Active hydrocarbon maturation during ore deposition will facilitate, and may be necessary for, MVT formation.

The gas pulsar hypothesis is a new proposal for MVT formation that, if correct, will cause us to look at MVT formation in a very different, much broader, and more integrated way. MVT deposits may be one consequence of gas in sub-water table pore space, but there are likely to be many others. Understanding the consequences of the capillary phenomena made possible by the burial of organic matter in significant quantities will require a great deal of work by many people over many years, but the effort is likely to be very productive in generating scientific understanding, new scientific hypotheses, and new concepts for resource exploration and exploitation.

ACKNOWLEDGEMENTS

An invitation from Dave Symons, Chairman of the Geofluids V organizing committee, to present a paper in a session with the theme 'Origin and evolution of fluids in the crust' caused me to think further on the topics described in this paper. I thank Dave and the organizing committee for motivating this work. I am also grateful to Iain Samson, David Deming, and an anonymous reviewer for suggesting ways the initial draft of this paper could be improved.

REFERENCES

Arbenz JK (1989) The Ouachita system. *Geology of North America, Geological Society of America*, **A**, 371–396.

Bear J (1972) *Dynamics of Fluids in Porous Media*. Elsevier, New York, 764 pp.

Behar E, Simonet R, Rauzy E (1985) A new cubic equation of state. *Fluid Phase Equilibria*, **21**, 237–255.

Berg RR (1975) Capillary pressures in stratigraphic traps. *American Association of Petroleum Geologists Bulletin*, **59**, 939–956.

Byrnes AP (2003) Aspects of permeability, capillary pressure, and relative permeability properties and distribution in low-permeability rocks important to evaluation, damage, and stimulation. *Rocky Mountain Association of Geologists-Petroleum Technology Transfer Council (RMAG/PTTC) Fall Symposium*, **2003**, 1–12.

Cathles LM (2001) Capillary seals as a cause of pressure compartmentation in sedimentary basins. *Petroleum Systems of Deep-Water Basins: Global and Gulf of Mexico Experience, Houston, Texas, GCSSEPM*, GCS 021, 561–571.

Cathles LM, Adams JJ (2005) Fluid flow and petroleum and mineral resources in the upper (<20 km) Continental Crust. *Society of Economic Geologists*, **100th** Anniversary volume, 77–110.

Cathles LM & Losh SL (2002) *Seal Control of Hydrocarbon Migration and its Physical and Chemical Consequences: Volume V: A Modeling Analysis of Hydrocarbon Chemistry and Gas Washing, Hydrocarbon Fluxes, and Reservoir Filling*. GRI-03/0065, Gas Research Institute, Chicago, IL, pp. 1–63.

Cathles LM, Chen Duo Fu, Nicholson B (2006) A dimensionless vent number characterizing the thermal impact of fluid discharge through planar and cylindrical vents with particular application to seafloor gas vents crystallizing hydrate. *Journal of Geophysical Research*, **111**, B10205, doi:10.1029/2005JB004221.

Cook TD, Bally AW (1975) *Stratigraphic Atlas of North and Central America*. Princeton University Press, Princeton, NJ.

Davis TB (1984) Subsurface pressure profiles in gas saturated basins. *American Association of Petroleum Geologists Memoir*, **38**, 189–203.

De Witt W (1986) Devonian gas-bearing shales in the Appelachian basin. *American Association of Petroleum Geologists Studies in Geology*, **24**, 1–8.

Deming D (1994) Factors necessary to define a pressure seal. *American Association of Petroleum Geologists Bulletin*, **78**, 1005–1009.

Earlougher RC (1977) *Advances in Well Test Analysis*. Society of Petroleum Engineers of the American Institute of Mining Engineers, New York.

Eisenlohr BN, Tompkins LA, Cathles LM, Barley M, Groves DI (1994) Mississippi Valley-type deposits: products of brine expulsion by eustatically induced hydrocarbon generation? An example from northwestern Australia. *Geology*, **22**, 315–318.

Erendi A, Cathles LM (2001) Gas capillary inhibition to oil production. *Petroleum Systems of Deep-Water Basins Global and Gulf of Mexico Experience, Houston, Texas, GCSSEPM*, GCS 021, 607–618.

Faure G (1977) *Principles of Isotope Geology*. John Wiley, New York.

Frakes LA, Francis JE, Syktus JI (1992) *Climate Modes of the Phanerozoic*. Cambridge University Press, Cambridge.

Freeze RA, Cherry JA (1979) *Groundwater*. Prentice Hall, New Jersey.

Goldhaber MB, Church SE, Doe BR, Aleinikoff JN, Brannon JC, Podosek FA, Mosier EL, Taylor CD, Gent CA (1995) Lead and sulfur isotope investigation of Paleozoic sedimentary rocks from the southern mid-continent of the United States: Implications for paleohydrology and ore genesis of the Southeast Missouri lead belt. *Economic Geology*, **90**, 1875–1910.

Hagni RD (1976) Tri-state ore deposits: the character of their host rocks and their genesis. In: *Handbook of Strata-bound and Strataform Ore Deposits*, Vol. 6 (ed. Wolf KH), pp. 457–494. Elsevier, New York.

Hanor JS (1997) Controls on the solubilization of lead and zinc in basinal brines. In: *Carbonate-hosted Lead–Zinc Deposits* (ed. Sangster DF), *Special Publication – Society of Economic Geologists*, **4**, 483–500.

Hutchinson I (1985) The effects of sedimentation and compaction on oceanic heat flow. *Geophys Journal. Royal Astronomical Society*, **82**, 439–459.

Law BE (2002) Basin-centered gas systems. *American Association of Petroleum Geologists Bulletin*, **86**, 1891–1919.

Leach DL, Symons DTA, Brannon J (2001) Mississippi Valley-type lead–zinc deposits through geologic time: implications from recent age-dating research. *Mineralium Deposita*, **36**, 711–740.

Masters JA (1979) Deep basin gas trap, western Canada. *American Association of Petroleum Geologists Bulletin*, **63**, 152–181.

Masters JA (1984) Lower Cretaceous oil and gas in western Canada. *American Association of Petroleum Geologists Memoir*, **38**, 1–33.

Meissner FF (1978) Petroleum geology of the Bakken Formation, Williston Basin, North Dakota and Montana. In: *The Economic Geology of the Williston Basin: Proceedings of the Montana Geological Society 24th Annual Conference* (ed. Rherig D), pp. 207–227. Montana Geological Society.

Muskat M (1937) *The Flow of Homogeneous Fluids Through Porous Media*. McGraw Hill, New York.

Revil A, Cathles LM (2001) The porosity-depth pattern defined by 40 wells in Eugene Island Aouth Addition, Block 330 Area, and its relation to pore pressure, fluid leakage, and seal migration. *Petroleum Systems of Deep-Water Basins: Global and Gulf of Mexico Experience, Houston, Texas, GCSSEPM*, GCS 021, 687–712.

Rowan EL, Goldhaber MB (1995) Duration of mineralization and fluid-flow history of the Upper Mississippi Valley zinc-lead district. *Geology*, **23**, 609–612.

Sangster DF, Nowlan GS, McCracken AD (1994) Thermal comparison of Mississippi Valley-type lead–zinc deposits and their host rocks using fluid inclusion and conodont color alteration index data. *Economic Geology*, **89**, 493–514.

Shosa JD, Cathles LM (2001) Experimental investigation of capillary blockage of two phase flow in layered porous media. *Petroleum Systems of Deep-Water Basins: Global and Gulf of Mexico Experience, Houston, Texas, GCSSEPM*, GCS 021, 721–740.

Silver C (1950) The occurrence of gas in the Cretaceous rocks of the San Juan basin, New Mexico and Colorado. *New Mexico Geological Society First Field Conference, San Juan Basin*, pp. 109–123.

Sverjenski DA (1981) The origin of a Mississippi Valley-type deposit in the Viburnum Trend, southeast Missouri. *Economic Geology*, **76**, 1848–1872.

Ungerer P, Behar E, Discamps D (1983) Tentative calculation of overall volume expansion of organic matter during hydrocarbon genesis for geochemistry data: implications for primary migration. *Advances in Organic Geochemistry*, 129–135.

APPENDIX A: CALCULATIONS

The discussion in the body of this paper rests on a relatively large number of simple calculations, which in turn depend on a relatively large number of parameters such as

compressibility, permeability, etc. These calculations are presented in this appendix. The parameters used are defined and assigned appropriate values in Table A1. The text refers to the calculations by the number of the appendix section. For example 'Appendix calculation 1' refers to the calculation of pressure drops across a 10 microdarcy parting in the paragraph immediately below. Where permeability is involved, the calculation is illustrated for a particular sediment permeability (whose results are given in bold), but results are also given, as a column vector, for three permeabilities: 0.1, 2.5, and 10 μD, where 1 μD is one microdarcy and equals 10^{-18} m^2. This provides a measure of how sediment permeability, the main controlling parameter, affects the operation of a gas pulsar. Each major equation is numbered. Table A1 references the equations that define or involve a particular parameter.

Pressure drops across a 10 microdarcy parting

Capillary pressure drops

The grain diameter, d, suggested by the Carmen–Kozeny relationship (Bear 1972; Freeze & Cherry 1979) for a sediment with permeability $k = 10^{-17}$ m^2 (10 microdarcy) and porosity $\phi = 0.2$ is 0.38×10^{-6} m:

$$k = \frac{d^2}{180}\frac{\phi^3}{(1-\phi)^2}. \tag{A1}$$

$$10^{-17} = \frac{d^2}{180}\frac{0.2^3}{0.8^2}, \quad d = 0.38 \times 10^{-6}.$$

The effective pore radius is $0.326d$ (Shosa & Cathles 2001), so assuming the coarse pores are large, the capillary entry pressure of gas, from Laplace's law (Bear 1972; Berg 1975) is:

$$\begin{aligned}\Delta P_c &= 2\gamma\left(\frac{1}{r_{fine}} - \frac{1}{r_{coarse}}\right)\\ &= 20 \times 0.03 \times \left(\frac{1}{0.326 \times 0.38 \times 10^{-6}}\right)\\ &= \left\{\begin{array}{l}\mathbf{4.8 \times 10^5\ Pa}\\ 9.6 \times 10^5\ \text{Pa}\\ 4.8 \times 10^6\ \text{Pa}\end{array}\right\}\begin{array}{l}10\,\mu\text{D}\\ @2.5\,\mu\text{D},\\ 0.1\,\mu\text{D}\end{array}\end{aligned} \tag{A2}$$

where r_{fine} is the effective radius of the fine pores, r_{coarse} is the effective radius of the coarse pores, and γ is the interfacial tension between water and gas. ΔP_c is both the entry gas pressure and the 'capillary pressure drop' discussed in this paper. The final results, here and for other calculations that involve permeability, are given in column vector form (curly brackets) for the three sediment permeabilities listed to the right of the vector. The result calculated is bold. In this case it is the result for 10 microdarcies because radius of the fine pores is estimated for this permeability.

Gas flow pressure drops

Once gas penetrates the partings, a gas flow rate $V_g = 10$ m year^{-1} will produce only a 0.007 MPa pressure drop, ΔP_g, across each parting if the thickness of the parting $w = 1$ cm and its permeability 10 μD:

$$\begin{aligned}\Delta P_g &= \frac{\mu_g V_g W}{k}\\ &= \frac{2.3 \times 10^{-5} \times \left(\frac{10}{3.15 \times 10^7}\right) \times 0.01}{10^{-17}}\\ &= \left\{\begin{array}{l}\mathbf{0.007\ MPa}\\ 0.028\ \text{MPa}\\ 0.7\ \text{MPa}\end{array}\right\}\begin{array}{l}10\,\mu\text{D}\\ @2.5\,\mu\text{D}.\\ 0.1\,\mu\text{D}\end{array}\end{aligned} \tag{A3}$$

Lithostatic and hydrostatic pressure at 4 km depth

Assuming the average density of sediments $\rho_{sed} = 2200$ kg m^{-3} and that the sediments will hydrofracture at $f_{hyd} = 0.8$ of lithostatic pressure, the maximum pressure that can be attained at a depth $D = 4000$ m, is:

$$P_{Fx} = \rho_{sed} g D f_{hyd} = 2200 \times 10 \times 4000 \times 0.8 = 70\,\text{MPa}. \tag{A4}$$

The subscript, Fx, indicates the pressure is the fracture pressure. Hydrostatic pressure at 4000 m is 40 MPa:

$$P_{whyd} = \rho_w g D = 1000 \times 10 \times 4000 = 40\,\text{MPa}. \tag{A5}$$

Here the subscript "whyd" indicates water hydrostatic. The maximum pressure in excess of hydrostatic that could drive fluid flow is thus:

$$\Delta P_{max} = P_{Fx} - P_{whyd} = 30\,\text{MPa}. \tag{A6}$$

Gas expulsion if Arkoma decompressed

The density of methane at 100°C and 70 MPa is approximately 263 kg m^{-3}, and at 100°C and 40 MPa it is approximately 193 kg m^{-3} (calculated from the Behar *et al.* 1985 equation of state). Conservation of mass requires that if methane is decompressed from 70 to 40 MPa, a volume of gas equal to 36% of the gas-filled porosity must be expelled. The volume of methane expelled equals the mass of methane expelled, ΔM, divided by the density of decompressed methane. The fraction of the pore volume expelled, X_g is this volume divided by the gas-filled sediment porosity:

$$\begin{aligned}X_g &= \frac{\Delta M}{\phi \rho_{CH4}^{T=100,P=40\text{MPa}}}\\ &= \frac{\phi\left(\rho_{CH4}^{T=100,P=70\text{MPa}} - \rho_{CH4}^{T=100,P=40\text{MPa}}\right)}{\phi \rho_{CH4}^{T=100,P=40\text{MPa}}}\\ &= \frac{\phi \rho_{CH4}^{T=100,P=70\text{MPa}}}{\phi \rho_{CH4}^{T=100,P=40\,\text{MPa}}} - 1 = 0.36.\end{aligned} \tag{A7}$$

The gas compressibility at 40 MPa is 1.6×10^{-8} Pa^{-1} and at 70 MPa is approximately 0.6×10^{-8} Pa^{-1} (Earlougher 1977; Behar *et al.* 1985, Appendix D). On average over the decompression the compressibility is 1.1×10^{-8} Pa^{-1}. Note that 1.1×10^{-8} Pa^{-1} times 30×10^{6} Pa equals 0.33, which is similar to 0.36 above. This is a check on, and an alternative derivation of, X_g.

Gas expulsion from Arkoma in 5000 years

Considering just the gas expansion due to decompression, the hydraulic diffusivity, κ_g of a gas-filled basin of 2.5 microdarcy permeability and 5% porosity is approximately 1.7×10^{-4} m^2 s^{-1}:

$$\kappa_g = \frac{k}{\phi C_g \mu_g} = \frac{2.5 \times 10^{-18}}{0.05(1.1 \times 10^{-8})(2.65 \times 10^{-5})} = \left\{ \begin{array}{l} 6.86 \times 10^{-4} m^2 s^{-1} \\ \mathbf{1.7 \times 10^{-4} m^2 s^{-1}} \\ 6.86 \times 10^{-6} m^2 s^{-1} \end{array} \right\} \begin{array}{l} 10\,\mu D \\ @2.5\,\mu\,D\,, \\ 0.1\,\mu D \end{array} \quad \text{(A8)}$$

where ϕ is the sediment porosity, C_g is the gas compressibility (from immediately above), and μ_g the gas viscosity (from Table A1). The distance into a basin-centered gas zone, ΔW, that will depressurize in 5000 years once the capillary seals fail can be estimated:

$$\Delta W = 2\sqrt{\kappa_g t} = 2\sqrt{(1.7 \times 10^{-4})(5000)(3.15 \times 10^{7})} = \left\{ \begin{array}{l} 20.8\,km \\ \mathbf{10.4\,km} \\ 2.08\,km \end{array} \right\} \begin{array}{l} 10\,\mu\,D \\ @2.5\,\mu\,D\,, \\ 0.1\,\mu\,D \end{array} \quad \text{(A9)}$$

where 3.15×10^7 is the number of seconds in a year. The decompression will be approximately linear across ΔW. The volume change of the gas will linearly decrease from 36% to 0%, the average volume change will be 18%, and 18% of the contained gas, or approximately 170 km^3, will be expelled from that portion of the 10.4 km wide edge of the 300 km long Arkoma basin that lies between 4 and 10 km depth:

$$\Delta V_g = L \Delta W T \phi \left(\frac{\Delta X_g}{2}\right) = 300 \times 10.4 \times 6 \times 0.05 \times \left(\frac{0.36}{2}\right) = \left\{ \begin{array}{l} 337\,km^3 \\ 168\,km^3 \\ 33.7\,km^3 \end{array} \right\} \begin{array}{l} 10\,\mu D \\ @2.5\,\mu D\,. \\ 0.1\,\mu D \end{array} \quad \text{(A10)}$$

If the sediment compacts after the pressure is reduced, additional gas will be expelled. Full compaction of a 4.2 wide × 4.2 km deep prism at the 300 km long edge of the gas zone could expel an additional 260 km^3 if the average porosity was initially 5%.

Pressure recovery time

The maturation of kerogen to gas is a positive volume reaction in which 1 volume of kerogen becomes approximately 2 volumes of gas (Meissner 1978; Ungerer *et al.* 1983). New gas is generated in the Arkoma basin at the rate the isotherms that define the conversion of kerogen to oil and oil to gas rise through the sedimentary strata, V_{GW}:

$$V_{gMat} = LWV_{GW}\Delta t G_k. \quad \text{(A11)}$$

Here, the plan area of the Arkoma is taken to be $L = 300$ by $W = 100$ km, V_{GW} is the rate of rise of the oil and gas windows due to thermal recovery from the basin cooling caused by the rapid deposition of Atokan sediments in km Ma^{-1}, Δt is the time required to mature V_{gMat}, and G_K is the kerogen grade (in volume percent organic matter, which is approximately the same as wt percent organic matter, as the densities of kerogen and sediments are similar). Assuming the top of the gas zone rises 3 km in 60 Ma, $V_{GW} = 0.05$ km Ma^{-1}, $G_K = 0.01$, and $V_{gMat} = 168$ km^3, $\Delta t = 10$ Ma.

A meltwater trigger for the gas pulsar?

Suppose a portion of the basin-centered gas zone is overlain by ocean. A 100 m rise in sea level, such as occurs in approximately 5000 years when continental glaciers melt, will load this part of the basin rapidly. A loading rate R_{SL} of 100 m seawater in 5000 years is equivalent to a sedimentation rate $S \sim 9$ km Myr^{-1}:

$$\rho_w g R_{SL} = \rho_{sed} g S, \text{ so } S = R_{SL}\frac{\rho_w}{\rho_{sed}} = \frac{100\,m}{5000\text{ years}} \times \frac{1000}{2200} = 9 \times 10^{-3}\ Myr^{-1}. \quad \text{(A12)}$$

If the gas cannot escape and porosity times the compressibility of the gas is substantially less than the compressibility of the shale matrix, i.e. $\phi C_g \ll C_{shale}$, the gas pressure will increase by nearly the melt water load. Long-term compaction (porosity change) occurs by pressure dissolution at grain contacts and re-deposition of the dissolved solid material on pore surfaces and is related to effective stress: $\Delta\phi = \Delta V_{shale}/V_{shale} = C_{shale}(\Delta P_{MW} - \Delta P_{gMW})$. But, $\Delta\phi/\phi = C_g \Delta P_g$. Substituting and rearranging we find:

$$\Delta P_{gMW} = \frac{\Delta P_{MW}}{1 + \phi C_g / C_{shale}}. \quad \text{(A13)}$$

As the compressibility of methane at the top of our hypothetical gas zone in the Permian Arkoma basin (at 100°C and 70 MPa) is 0.65×10^{-8} Pa^{-1} and decreases with depth, $\phi = 0.05$, and $C_{shale} = 1.4 \times 10^{-8}$ Pa^{-1}, $\phi C_g \ll C_{shale}$ and $\Delta P_g \approx \Delta P_{MW}$. The gas pressure in the

pores of the gas zone that underlie ocean will increase by essentially the full meltwater load $\Delta P_{MW} = 1$ MPa. Further discussion of compaction can be found in Revil & Cathles (2001).

A rapid injection of a large volume of gas into an aquifer could be triggered if the increase in gas pressure produced by the melt water load can be transmitted to the capillary seals that separate the gas zone from the aquifer. From the previous discussion in this Appendix, the rate at which a pressure changes can be transmitted depends on how far the meltwater-loaded part of the gas zone is from the aquifer contact, and the permeability of the more permeable pathways to this contact. From equation (A9) pathways with permeability >10 μD will be needed if the loaded zone is 20 km from the aquifer contact. If the loaded parts of the gas zone are 200 km distant, pathways one hundred times more permeable will be needed (millidarcy permeability). Thus, for meltwater loading to trigger a gas pulsar, portions of the gas zone of the basin will probably need to have relatively high permeability network that connects the loaded part of the gas zone to the boundary between the gas zone and the aquifer.

Table A1 Definition and selected values of parameters used in the calculations presented in this appendix and paper.

Parameter	Definition	Value	Reference
α[-]	$= \log_{10} \frac{4t\kappa}{W_{cyl}^2}$		Parameter in Ω
C_{shale} [Pa^{-1}]	Long-term compressibility of un-compacted sediments	1.4×10^{-8}	Revil & Cathles (2001)
C_g [Pa^{-1}]	Compressibility of methane gas at 100°C and 40 and 70 MPa	1.64×10^{-8} 0.65×10^{-8}	Earlougher (1977)
d [m]	Diameter of grains in sand		
D [km]	Depth of basin	10 (Arkoma)	
ϕ [–]	Sediment porosity	0.4 to <0.05	
$\Delta\phi$[–]	Compactive change porosity		
g [m sec^{-2}]	Gravitational acceleration	9.8	= 10 in calculations
γ [N m^{-1}]	Water–gas interfacial tension at 40 MPa and 100°C	~0.03	Estimated from Berg (1975), Figure 7
k [m^2]	Permeability (10^{-18} m^2 = 1 μD)		
K [W m^{-1} °C^{-1}]	Thermal conductivity sediment	1.5	
κ [m^2 sec^{-1}]	Thermal diffusivity	$= \frac{K}{\rho_m c_m}$	Parameter in α
κ_g [m^2 sec^{-1}]	Hydraulic diffusivity	$= \frac{k}{\phi C_g \mu_g}$	Equation (A8)
L [km]	Length of a basin	300 (Arkoma)	
μ_g [Pa sec]	Viscosity of gas at 100°C and 40 and 70 MPa	2.3×10^{-5} 3×10^{-5}	Earlougher (1977)
μ_w [Pa sec]	Viscosity of water at 100°C > 40 MPa pressure	0.5×10^{-3}	
ρ_{sed} [kg m^{-3}]	Average density of basin sediments	2200	
ρ_w [kg m^{-3}]	Density of water	1000	
N_v [–]	Vent number	$= \frac{W_{cyl} N_{Pe}}{4d^2\Omega} \sqrt{\pi\kappa t}$	Cathles *et al.* (2006)
N_{Pe} [–]	Peclet number	$= \frac{\rho_f c_f V d}{K}$	Parameter in N_v
P_{Fx} [Pa]	Fracture pressure		Equation (A4)
P_{whyd} [Pa]	Water hydrostatic pressure		Equation (A5)
P_g [Pa]	Pressure of gas in basin		
ΔP_c [Pa]	Capillary entry pressure		Equation (A2)
ΔP_f [Pa]	Pressure drop across parting due to fluid flow		Equation (A3)
ΔP_{max} [Pa]	Maximum possible pressure in excess of hydrostatic		Equation (A6)
ΔP_{MW} [Pa]	Increase surface pressure due to melt water rise in sea level		
ΔP_{gMW} [Pa]	Increase in P_g caused by melt water load		Equation (A12)
R_{SL} [m yr^{-1}]	Rate of rise in sea level		
S [km Myr^{-1}]	Sedimentation rate		Equation (A12)
S_w [–]	Fraction of pore space filled with water		Figure 2
S_{iw} [–]	Irreducible water saturation		Figure 2
$\rho_w c_w$ [J m^{-3} °C]	Volume heat capacity of pore water	4.18×10^6	
$\rho_m c_m$ [J m^{-3} °C]	Volume heat capacity of sediment	2.45×10^6	
T [km]	Basin thickness below 4 km	6 (Arkoma)	Equation (A10)
V [m sec^{-1}]	Darcy flux of fluid in flow tube		
V_{gMat} [km Ma^{-1}]	Upward velocity gas window	0.05	If double heat flow in 60 *Ma*
V_{shale}	Volume of shale		
ΔV_{shale}	Change in volume of shale due to compaction		
ΔV_g [km^3]	Volume of gas expelled from basin	Calculated	Equation (A10)
V_{GW} [km^3]	Maturation gas volume	Calculated	Equation (A11)
W_{cyl} [m]	Diameter of flow tube	m	Parameter in N_v

Table A1 Continued

Parameter	Definition	Value	Reference
W [km]	Width of a basin	100 (Arkoma)	
ΔW [km]	Depressurized width of basin	Calculated	Equation (A9)
Ω [–]	Polynomial in α		Parameter in N_v
X_g [–]	Fraction of gas expelled from pores		Equation (A7)